2. Introduction

Bioactive glasses (BGs) are orthobiologic materials which are widely employed as a bone graft for the regeneration of bone defects caused as a result of trauma or various diseases (Hoppe, Güldal et al. 2011). 45S5 is the FDA-approved BG which is mostly used as a coating over orthopedic implants for bone joining (Ajita, Saravanan et al. 2015). They are also preferred as dental fillings as they increase the pH which imparts bactericidal properties (Earl, Leary et al. 2011, Jones 2015). Normally, traumatic injuries like bone fractures and tissue damage are associated with inflammation which is considered to be the primary pathological hallmark (Lonergan, Baker et al. 2003). Therefore, there is a need to develop a novel BG with minimum immunogenic response for improved biological application. Further, some of the studies suggested the orthobiologic biomaterials that are employed as a bone graft are associated with inherent limitations of immune rejection and inflammation (Kneser, Schaefer et al. 2006, Mariani, Lisignoli et al. 2019). This immune response is mediated due to the activation of calcium-dependent immunogenic pathways even in the absence of immune-stimulating signals due to their physiochemical properties (Andorko and Jewell 2017). Hence, it we have investigated the effectiveness of BG on various inflammatory mediators.

BG is mostly limited to orthopedic and dental purposes as it stimulates osteoblast proliferation but there are some reports on its use in healing damaged soft tissues (Rahaman, Day et al. 2011). Basically, acute inflammation, an initial step during the healing of any injury, facilitates tissue remodeling (Dong, Chang et al. 2017) which subsides within a few days after the insult. However, biomaterials induce excessive expression of pro-inflammatory cytokines due to the activation of the resting immune

cells of the brain i.e. M1 phenotype of microglia has a deleterious effect on tissue regeneration and limits their use (Boehler, Graham et al. 2011). So, there is a need to develop a bioactive material that would have minimal effect on the release of inflammatory mediators from the glial cells without causing cytotoxicity.

Growing evidence suggests that doping of various trace metals like Cu^{2+}, Mg^{2+}, Zn^{2+}, and Sr^{2+} has various pharmacological effects that enhance the biological performances of BGs. Similarly, previous reports from our laboratory highlighted that doping barium in the BG framework has the potential to treat ulcers by forming a protective layer in the stomach against abrasive luminal acids (Paliwal, Kumar et al. 2018). Barium is also reported to generate a barium spike in the growth cone of the regenerating axon (Macvicar's and Llinas 1985). Like calcium, barium is one of the trace alkaline earth metals found in the human body and is enriched in the enamel of the teeth (Austin, Smith et al. 2013). The enrichment of barium in the bone of rodents is also reported and is essential for their calcification (Moore Jr 1964). There are various reports on the use of barium as a radiocontrast agents as well as in radio-osteometric analysis (Madanat, Moritz et al. 2009). Moreover, barium causes concentration-dependent contraction of the smooth muscle (Satoh, Kubota et al. 1987) but there is a paucity of information on the pharmacological potential of barium. However, there is constrained information on the use of barium-doped bioglass on pro and anti-inflammatory markers which are generally released during tissue injury. Based on the consolidated evidence on barium, in the present study, we incorporated barium in BG (BaBG) and investigated its effects on the pro-inflammatory cytokines released during traumatic events.

BGs are mostly prepared using the traditional method of melting or quenching silica and alkali oxides at very high temperatures (Hench 2006). However, these alkali

ingredients pick up other impurity cations at a very high temperature which reduces the binding of the bone tissues with the bioglass and sometimes causes hypersensitivity (Li, Clark et al. 1991). The final steps of grinding, polishing, and sieving the bioglass add further contaminants to it. Therefore, there is a need to use an alternate method which can reduce impurity and enhance its biocompatibility and application. The sol-gel method is a wet-chemistry process that produces porous bioglass with an increased surface area that makes bioglass to be used as a carrier of drugs for controlled release (Zheng and Boccaccini 2017). The sol-gel-derived BG has a faster rate of dissolution in the body fluid that stimulates the formation of the hydroxyapatite (HA) on the surface of BGs (Li, Clark et al. 1991, Pereira and Hench 1996). Moreover, the release of various ions upon dissolution elicits local therapeutic action and thus has the potential to be used in soft tissue engineering (Baino, Fiume et al. 2018). In the light of above-mentioned facts, the BaBG was prepared using the sol-gel method.

To validate our hypothesis, BaBG and 45S5 were prepared in the nanometer range following the sol-gel method. 45S5 being the FDA-approved biomaterial, was used as a positive control for all the biological *in vitro* experiments and also to investigate the effect of barium on various biological activities. The structure of BGs was characterized using Fourier transform infrared spectroscopy (FTIR) and X-ray diffractometry (XRD) and the surface phenomenon was assessed using scanning electron microscopy (SEM). The cytotoxicity of BaBG and 45S5 was assessed by MTT on the C6 and K562 cell lines. The cell-cell interaction was checked by the scratch assay which is an *in vitro* transection model of neurotrauma. Further, the biocompatibility was confirmed by the hemolysis test and the *in vitro* bioactivity by immersing the BGs samples in SBF. In addition, the immune response of BaBG and 45S5 was evaluated by measuring the pro-

inflammatory cytokines like interleukin (IL-6) and tumor necrosis factor (TNF-α) as well as the anti-inflammatory IL-10. As BaBG has never been considered before as a reinforcing compound to bind with the peripheral tissue, the BG developed in the present study is a newer bioactive material for biomedical engineering applications.

2.1. Materials and Methods

2.1.1. Synthesis of the bioactive glasses

2.1.1.1. Barium doped Bioactive glass (BaBG)

BaBG (44.85SiO_2-2.6P_2O_5-24.3Na_2O-26.9CaO-1.35BaO) (mol%) was prepared using the analytical grade chemicals through the sol-gel method (Long, Yang et al. 2015). To prepare 10 g of glass, 15.97 ml tetraethyl orthosilicate (TEOS) and 1.41 ml triethyl phosphate (TEP) (from SRL Pvt. Ltd., India) were weighed and stirred for 45 minutes for homogenous mixing. Then to induce catalytic hydrolysis, 10.21 g calcium nitrate tetrahydrate ($Ca(NO_3)_2.4H_2O$, 99%), 6.64 g sodium nitrate ($NaNO_3$, 99%) and 0.58 g barium nitrate ($Ba(NO_3)_2$, 99%) (all from Loba Chemie, Mumbai, India) are dissolved in 150 ml of water/ethanol mixture in acidic pH. Then the above-nitrated solution was gradually added into the silica-phosphate solution and constantly stirred for 2 h at 40°C. The solution was then aged for a period of 24 h at room temperature. The aged gel was dried at a temperature of 60°C for 24 h and further at 120°C for another 24 h to remove excess water. The dried sample was grounded and thermally treated at 550°C for 6 h in an oxidizing environment at 3°C/ min in an electric furnace to remove residual nitrates from precursors of calcium, sodium, and barium. At last, the sintered samples were pulverized in a zirconia planetary ball mill (VB ceramics, India) for 15 min at 500 rpm to make a fine powder.

2.1.1.2. 45S5

The sol-gel method was used to synthesize 45S5 (46.1SiO_2-2.6P_2O_5-24.4Na_2O-26.9CaO) (mol%) involving hydrolysis and the polycondensation reactions (Pirayesh and Nychka 2013). 10 g of the sol-gel derived bioglass was prepared by magnetic stirring 16.75 ml TEOS and 1.44 ml TEP (from Otto chemika) in the presence of ethanolic solution containing 1(M) nitric acid for 45 min. Subsequently, the following reagents were added to the above reaction mixture: 10.42 g calcium nitrate tetrahydrate and 6.81 g sodium nitrate (Loba Chemie, Mumbai, India) at an interval of 30 min with constant stirring. Now the above mixture was aged for 24 h and dried at 120°C for another 24 h to remove excess water. The dried gel was grounded and stabilized in an electric furnace at 550°C for 6 h to eliminate the residual nitrates from precursors of calcium and sodium. Finally, the fine powdered sample was obtained using a planetary ball mill (VB Ceramics, India).

Table 2.1. The chemical composition (mol %) of 45S5 and BaBG

Composition (Mol %)	45S5	BaBG
SiO_2	46.1	44.85
P_2O_5	2.6	2.6
Na_2O	24.4	24.3
CaO	26.9	26.9
BaO	0.0	1.35

2.1.2. Characterization of the bioactive glass samples

2.1.2.1. Particle size and surface area determination

The mean particle size of the synthesized bioactive glass samples was analyzed based on the principle of dynamic light scattering using distilled water as a dispersant at 25°C (Delsa™Nano C, Beckman Coulter, USA) (Patel, Surekha et al. 2019). The N_2

adsorption-desorption measurements were carried out (Quantachrome Instruments NOVA 1000, USA) and the BET-specific surface area, pore diameter, and pore volume were calculated using the Brunauer–Emmett–Teller (BET) and Barrett-Joyner-Halendra (BJH) methods (de Souza Balbinot, Leitune et al. 2020).

2.1.2.2. X-Ray Diffraction (XRD)

The phase analysis of the BG samples before and after the SBF (simulated body fluid) treatment was determined by X-ray diffraction (Ali, Ershad et al. 2018). The bioactive glass samples before and after 1, 3, 7, and 14 days of the bioactivity test were finely grounded and were subjected to X-Ray source to produce diffraction (RIGAKU-Miniflex II diffractometer). The source of radiation is Cu-Kα of wavelength (λ) =1.540 Å at 40 kV and 35 mA. The entire analysis was performed in 2θ ranging from 20° to 80° with a step size of 0.02° and the scanning speed was set at 1° per min. In this experiment, the interpretation of the XRD pattern obtained was referred using the JCPDS-International Centre for Diffraction Data cards.

2.1.2.3. Fourier Transform Infrared (FTIR) Spectroscopy

The analysis of the HCA developed over the bioactive glass samples which confirms the *in vitro* bioactivity was analyzed through FTIR spectrophotometer (FTIR-8400S, SHIMADZU) in the range of 400-4000 cm^{-1}. The finely powdered bioactive glass samples both before and after the SBF treatment for 1, 3, 7, and 14 days were mixed with the spectroscopic grade KBr in the ratio of 1:100 and were transferred to the die cavity. Then a pressure of around 10 MPa was applied to form a clear homogenous disc. This disc was then immediately placed inside the FTIR spectrophotometer, and the IR absorption spectra were recorded (Yadav, Singh et al. 2020).

2.1.2.4. Transmission electron microscopy (TEM)

The morphologies of 45S5 and BaBG were observed using a transmission electron microscope (TEM) (Tecnai G2, FEI Company, USA), and the phases present in the samples were detected by selected area electron diffraction (SAED).

2.1.3. Preparation of SBF (Simulated Body Fluid)

The *in vitro* bioactivity of the BG samples was checked using the SBF having a similar ionic concentration as the human plasma (Kokubo and Takadama 2006). NaCl, $NaHCO_3$, KCl, K_2HPO_4, $MgCl_2$, $CaCl_2$, and Na_2SO_4 were weighed and dissolved in the distilled water and the pH was adjusted to 7.4 using TRIS (trihydroxy methyl aminomethane) and 1N HCl at 37°C.

2.1.4. pH behavior of 45S5 and BaBG in SBF

The SBF treatment of the BG stimulates the formation of the hydroxyapatite (HA) and leaching out of the ions. BaBG and 45S5 were soaked in SBF in an airtight container held at 37°C at a concentration of 1.5 mg/ml for a period of 30 days. The changes in the pH of the SBF were measured in accordance with the method of Technical Committee 4 (TCO4) of the International Commission on Glass (ICG) (Macon, Kim et al. 2015).

2.1.5. *In vitro* hydroxyapatite forming ability of BaBG and 45S5

The BGs prepared can be assessed *in vitro* for their bioactivity (HA or HCA formation) by treating them with the SBF at a fixed concentration of 1.5 mg/ml and incubating it at 37°C according to Technical Committee 4 (TCO4) of the International Commission on Glass (ICG) (Macon, Kim et al. 2015). After the samples were soaked in the SBF for various periods up to 14 days, they were washed with deionized water and dried in the

hot air oven at 50°C for 5 h. The hydroxyl carbonated apatite (HCA) thus formed over the surface of BaBG and 45S5 are assessed by FTIR, XRD, and SEM-EDX (Tripathi, Kumar et al. 2016).

2.1.6. Surface characterization and quantitative elemental analysis of BaBG and 45S5

The change in the surface characteristics and elemental composition of the BG both before and after dispersing in the SBF can be analyzed by SEM and EDX (Energy-dispersive X-Ray) respectively. At first, the bioactive glass samples were treated with SBF for 1, 3, and 14 days at 37°C. Then the samples were rinsed thoroughly, dried at 50°C for 4 h and gold-coated using a sputter coating instrument. The changes in the composition of elements and surface morphology were assessed using the EVO/18 Research, ZEISS (Shahrbabak, Sharifianjazi et al. 2019).

2.1.7. Hemolysis assay

The blood compatibility of the BaBG and 45S5 can be evaluated by determining the percentage of hemolysis occurring when the heparinized blood is treated with bioactive glass samples. The hemolysis assay was performed as per the standard protocol (ASTM F 756-00) (ASTM 2000). 7 ml of PBS was taken in a test tube to which 5-100 mg of the powder (5, 10, 25, 50, and 100 mg) was added. Then 1ml of the heparinized blood was added to the above and incubated at 37 °C for 3 h. Positive and negative control was prepared by adding 7 ml of distilled water and 7ml of PBS to the heparinized blood respectively. Then the above solution was centrifuged at 10^4 rpm for 15min, and the optical densities of the supernatant were measured at 540 nm using a Micro-plate reader (BioTek, USA). The percentage of the hemolytic index was calculated by the following

formulae:

$$\text{Hemolytic index (\%)} = \frac{(\text{OD of sample} - \text{OD of negative control})}{(\text{OD of positive control} - \text{OD of negative control})} \text{ X } 100$$

2.1.8. Cell line and cell culture

Human erythromyeloma cells (K562; suspension type) were purchased from ATCC, Manassas, USA and the C6 (Rat glioblastoma; adherent type) cells were procured from NCCS, India. The cell lines were grown in a complete media containing RPMI 1640 (Invitrogen, Carlsbad, CA) supplemented with 10 % FBS (HiMedia, India), 100 U/ml penicillin and 100 µg/ml streptomycin (HiMedia, India).

2.1.9. *In vitro* cytotoxicity assay

Cytotoxicity assays are mostly performed with the aim to evaluate the cytocompatibility of the biomaterials for their biological use. The cytotoxic effect of BaBG and 45S5 was first assessed on the human leukemic suspension-type cells i.e. K562 cells to check their biocompatibility with the blood cells. The assay is based on the lytic activity of BaBG and 45S5 using CytoTox assay kit (Promega, USA) (Ali, Ershad et al. 2018). K562 cells tumor cells (5×10^3) were co-cultured with different range of concentrations (5-100 µg/mL) of BaBG and 45S5 in a 96-well culture plate and were incubated for 18 h at 37 °C, 5 % CO_2. The percentage of cytotoxicity was calculated from the undermentioned formula:

$$\%\ \text{Cytotoxity} = \frac{(\text{Experimental} - \text{Effector Spontaneous} - \text{Target Spontaneous})}{(\text{Target Maximum} - \text{Target Spontaneous})} \text{X} 100$$

The Target maximum refers to the positive control for cytotoxicity, Target spontaneous indicates negative control and the effector spontaneous is the treatment with bioactive glass.

2.1.10. Apoptosis assay (AO/EtBr)

The *in vitro* cytotoxicity of BaBG and 45S5 was further assessed on the adherent-type cells i.e. C6 cells by the apoptotic cell death assay using Acridine orange/Ethidium bromide staining under a fluorescence microscope (NikonEclipse80i, Nikon, Japan). The C6 cells are the glioblastoma cell line and were used as glial cells are the resting immune cells of the brain and their activation secretes various pro-inflammatory cytokines.

2.1.11. *In vitro* cell growth/proliferation assay

To access the growth inhibitory potential of BaBG and 45S5, the MTT assay was performed on both suspension as well as adherent-type cells i.e. K562 and C6 cells respectively. K562 cells (5×10^3 cells) were cultured in a 96-well culture plate and were treated with serial concentrations (5-100 µg/mL) of the BaBG and 45S5 and incubated for 48 hours at 37 °C in humidified condition (5 % CO_2). In the case of the C6 cells, 50 µg/mL of BaBG and 45S5 were plated in a 96-well plate and incubated for 24, 48, 72, and 96 hours followed by cell MTT assay using CellTiter 96 kit (Promega, USA). The absorbance (OD values) was measured at 570 nm using a microplate reader (BioTek, USA) (Hira, Mishra et al. 2014). The percent growth inhibition of the tumor cells was calculated using the mentioned formula:

$$\%\ \text{Growth Inhibition} = \left[1 - \frac{\text{Experimental OD570}}{\text{Target OD570}}\right] \text{X } 100$$

The Experimental OD value refers to 45S5 and BaBG-treated tumor cells while the Target OD indicates the corresponding values of the cells cultured in the absence of BaBG and 45S5.

2.1.12. Scratch-wound healing assay

Scratch assay, *in vitro* transection model for neurotrauma was performed on the C6 cells that were grown in the serum-free media and the wound was created by scratching the confluent layer of cells using the sterile microtip and the image was captured (0 h) (Zeng, Han et al. 2015). Then the cells were grown in the presence of BaBG, 45S5 (50µg/mL), and Temozolomide (TMZ) for 24 h and the wound images were photographed in a time-dependent manner (magnification 100X). The wound area was calculated automatically by CellProfiler™ image analysis software which quantifies the area occupied by the cell sample. The closure percentage increased as the cells migrated over time:

$$\text{Wound Closure } \% = \left[\frac{A(t = 0h) - A(t = \Delta h)}{A(t = 0h)}\right] X100$$

Where, A(t=0h) is the wound area at t=0 h and A(t=Δh) is the wound area measured hours after the scratch was performed.

2.1.13. Evaluation of the anti-inflammatory activity of bioactive glasses against LPS-induced inflammation

The anti-inflammatory effects of the BaBG were performed specifically on C6 cells as microglia mostly produce pro-inflammatory mediators in response to traumatic stimuli. The inflammation was induced in C6 cells (5×10^3) by incubating them with LPS (10 µg/mL) for 24 h at 37 °C, 5 % CO_2. In order to evaluate the anti-inflammatory effect of

BaBG and 45S5 against LPS-induced inflammation, the tumor cells were co-cultured with increasing concentrations of BaBG and 45S5 in a 96-well culture dish (0.1-100 µg/mL). The levels of IL-6, TNF-α and IL-10 were assessed through ELISA kit (Cat. No. E-EL-R0015, R0019, and R0016 respectively, Elabscience, USA) as per the manufacturer's guidelines.

2.1.14. Data Analysis

All the data was analyzed by Graph Pad Prism software (San Diego, CARRID: SCR_002798). The parameters performed on the cell lines and the hemolysis assay were analyzed by two-way ANOVA. Bonferroni post hoc test was performed on the significant data to observe the within and between group interaction. $P<0.05$ was considered to be significant in all the analyses and the values were presented as mean ± SD.

2.2. Results and Discussion

2.2.1. Particle size and surface area analysis

The prepared batches of BaBG and 45S5 bioactive glass had particle size in the nanometer range of 508 ± 39.3 nm and 430 ± 41.9 nm respectively. **Figure 2.1** represents the nitrogen adsorption-desorption isotherm plots of BaBG and 45S5 based on the amount of nitrogen physioabsorbed on the bioactive glass samples at varying relative pressure. The isotherm exhibited the presence of a hysteresis loop as previously observed (Taherkhani and Moztarzadeh 2016). The BET results are summarized in **Table 2.2** and the BET-specific surface area of 45S5 and BaBG are 20.271 and 18.029 m^2g^{-1} respectively that corroborated by their particle size. Further, the pore diameter of 45S5 and BaBG was 3.455 and 3.451 nm respectively. Therefore, according to the

IUPAC classification, it can be inferred that the pore size of the synthesized BGs is in the mesoporous range (pore diameter in between 2 to 50 nm). Thus, owing to its smaller particle size in the nanometer range these glass samples have a larger surface area which increases its biomedical applications.

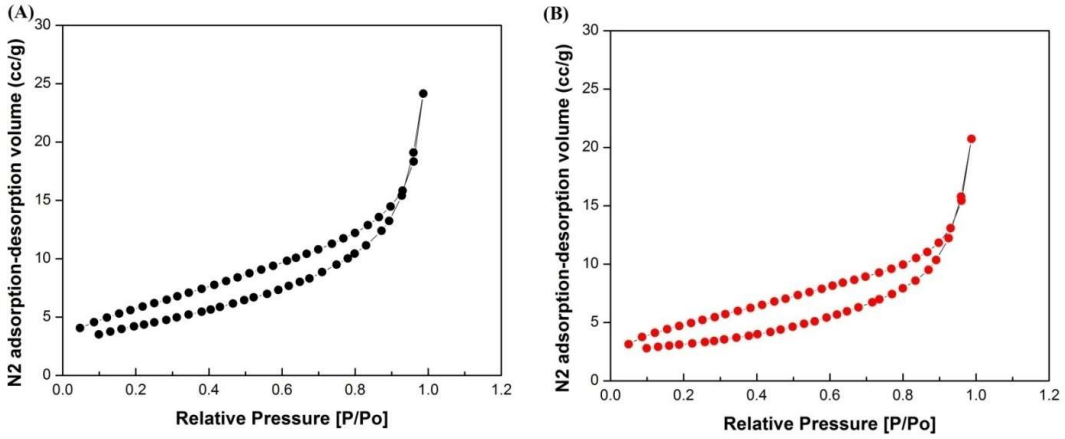

Figure 2.1: Nitrogen adsorption-desorption isotherm of (A) 45S5 and (B) BaBG at STP (standard temperature and pressure)

Table 2.2: Brunauer–Emmett–Teller (BET) analysis results of 45S5 and BaBG.

Material	BET-specific surface area (m^2/g)	Total pore volume (cc/g)	Pore diameter (nm)
45S5	20.371	In adsorption: 0.031	In adsorption: 3.455
		In desorption: 0.034	In desorption: 3.350
BaBG	18.029	In adsorption: 0.027	In adsorption: 3.457
		In desorption: 0.030	In desorption: 3.616

2.2.2. X-ray diffraction (XRD) analysis of BaBG & 45S5

The XRD patterns of 45S5 and BaBG before and after treating the samples in SBF for various time periods are shown in **Figure 2.2(A) and 2.2(B&C)** respectively. From **Figure 2.2(A)**, the amorphous nature of the bioactive glasses can be elucidated by the presence of a broad hump for both samples (45S5 and BaBG) in 2θ ranging from 20° to 30° which may be attributed to the Si-O-Si network (Fredholm, Karpukhina et al.

2010). Further, there are no prominent sharp peaks detected which confirms the amorphous nature of the samples. The SBF treatment of BaBG and 45S5 for 1, 3, 7 and 14 days shows a clear indication of crystalline peaks in the XRD patterns as depicted in **Figure 2.2 (B&C)**. This confirms the ability of the glasses to form hydroxyapatite (calcium phosphate hydroxide) in the presence of the body fluids which affirms the bioactivity of these samples (Ali, Ershad et al. 2018). In the present study, it is evident from the XRD pattern that in 45S5, there is presence of a prominent sharp peak of high intensity at $2\theta = 29.5°$ (PDF # 85-1108) which corresponds to calcite ($CaCO_3$) formation. Further, other sharp intense peaks that correspond to HA are formed at 2θ = 31.9°, 33.18°, 39.69°, 45.72 and 48.4° of *hkl* planes (211), (112), (212), (203) and (222) respectively (PDF # 74-0566) (Arepalli, Tripathi et al. 2016). This finding is supported by previous reports, where 45S5 favored the formation of calcite as the major phase during the HA layer growth due to the reaction of the excess calcium ions released with the carbonate ions present in the SBF (Kansal, Goel et al. 2011, Tulyaganov, Makhkamov et al. 2013). The calcite layer formed in 45S5 hampered the formation of HA but has the equal ability to bind to the bones and aid in its regeneration (El-Gohary, Tohamy et al. 2013). A series of studies reported various factors facilitating the formation of calcite, including the glass composition, particle size and porosity of the bioactive glasses (Mozafari, Banijamali et al. 2019). It is reported that highly porous bioactive glasses allow easy diffusion of Ca^{2+} ions that may ease the precipitation of calcite. Further, the bioactive glasses with increased surface area also promote greater leaching out of Ca^{2+} ions and thus facilitate the formation of calcite. Moreover, in our study, though calcite retarded the HA formation but this did not affect the biocompatibility of the bioglass as corroborated by the hemolysis and cytotoxicity

studies (**Figures 2.7 & 2.8**). Further, after 3 days of treatment with SBF, the diffraction pattern shows the formation of two prominent peaks at 2θ = 31.84 and 45.72 as depicted in **Figure 2.2(B)**.

Similarly in BaBG, the treatment with SBF led to the formation of the peak at a 2θ = 22.8°, 25.9°, 32°, 39° and at around 47.3° that corresponds to the precipitation of the hexagonal crystalline hydroxyapatite ($Ca_{10}(PO_4)_6(OH)_2$) (PDF #74-0566) (Arepalli, Tripathi et al. 2015). The intensity of the HA peak increased gradually with the increasing time duration of SBF treatment which corroborates the SEM result (**Figure 2.5**) and thus demonstrated the gradual increase in the HA formation. The above-mentioned peaks are associated with *hkl* (111), (002), (211), (212), and (222) reflecting planes. In addition, there was a formation of rhombohedral calcite in BaBG with a diffraction peak at 2θ = 29.5° matched with PDF #85-1108 (**Figure 2.2(C)**) (Tulyaganov, Makhkamov et al. 2013). The formation of calcite may be due to the addition of modifier cations of larger radii in the glass composition (Ba^{2+}; ionic radius = 135 pm) substituting for Ca^{2+} (ionic radius = 100 pm) (Mozafari, Banijamali et al. 2019). It is reported that ions of larger ionic radius tend to make the glass network less compact and hence the higher dissolution rate and more release of ions. Moreover, this trend was also observed by Arepalli et al., (Arepalli, Tripathi et al. 2015) but the inclusion of increasing concentration of barium ion reduced the calcite formation. Nevertheless, calcite is biocompatible and is reported to treat bone defects that emerge due to traumatic conditions or congenital defects (Monchau, Hivart et al. 2013) and the HA formed also facilitates the rapid proliferation of the osteoblast cells by initiating the production of ostegenin, a protein which helps in bone reconstruction (Ripamonti, Ma et al. 1992).

2.2.3. FTIR analysis of the bioactive glasses

Fourier transform infrared transmission spectra (in the range of 400-4000 cm^{-1}) of 45S5 and BaBG before and after immersion in the SBF solution for different time periods are shown in **Figure 2.3(A)** and **2.3 (B&C)** respectively. The transmittance spectra of BaBG and 45S5 illustrate bands centered at around 470 cm^{-1} and 793 cm^{-1} which corresponds to Si-O-Si symmetric bending and Si–O–Si symmetric stretching of non-bridging oxygen atoms between SiO_4 tetrahedral networks of the bioactive glasses respectively with very little differences in it (Tripathi, Hira et al. 2015). This also confirms that the bioactive glass samples have a tetragonal Si-O-Si group formed as a result of the polymerization of the silanol groups as reported previously (De Oliveira, De Souza et al. 2013). The peak observed at around 1096 cm^{-1} is associated with Si–O–Si asymmetric stretching [35]. The small band at around 1386 cm^{-1} is affirmed to the stretching mode of C–O vibration of CO_3 groups which may be formed due to the contact of the BaBG and 45S5 with CO_2 of the atmosphere (Yadav, Singh et al. 2020). The band centered at around 3489 cm^{-1} is mainly attributed to the OH group present on the surface of the bioactive glass samples.

Moreover, the *in vitro* bioactivity of the synthesized BaBG and 45S5 was assessed after soaking the bioactive glass samples in SBF for a period of 1, 3, 7, and 14 days. It is evident from **Figure 2.3(B)** that when the 45S5 sample was soaked in the SBF solution, newer divided vibrational bands were visible at around 571 and 616 cm^{-1}. This corresponds to the P–O bending mode of vibrations which corroborates the XRD and SEM results (**Figure 2.5**) and hence proves the precipitation of crystalline apatite (Deliormanlı 2016). An additional peak was observed at around 974 cm^{-1} which is

attributed to the symmetrical stretching of the P-O bond (Tripathi, Kumar et al. 2016). The bands at around 1492 and 1631 cm^{-1} correspond to the (carbonate) C–O stretching mode of the CO_3^{2-} group formed due to exposure of bioglass sample to the environmental CO_2 or precipitation of the crystalline phase of calcite as confirmed by XRD (Pazarçeviren, Tahmasebifar et al. 2018). A very broad peak at around 3467 cm^{-1} was observed which can be attributed to the O-H stretching mode of vibrations thus confirming the formation of hydroxy carbonated apatite (HCA) (Ravarian, Moztarzadeh et al. 2010). Similarly, BaBG after the SBF treatment showed two divided vibrational bands at around 573 and 623 cm^{-1} which corresponds to P-O bending (De Oliveira, De Souza et al. 2013) (**Figure 2.3(C)**) that confirms the formation of crystalline calcium phosphate (hydroxyapatite) layer on the surface as supported by SEM & XRD results. The band observed at around 1095 cm^{-1} is due to PO_4^{3-} bending and 1639 cm^{-1} corresponds to the carbonate groups CO_3^{2-} indicating the precipitation of carbonated apatite (HCA) similar to the apatite formed in the bones (Macon, Kim et al. 2015). Even the band observed at 3448 cm^{-1} is due to the presence of a hydroxy group on the surface of BaBG. Hence, based on the FTIR study we can conclude that BaBG and 45S5 favor the formation of hydroxy carbonated apatite layer following treatment with SBF.

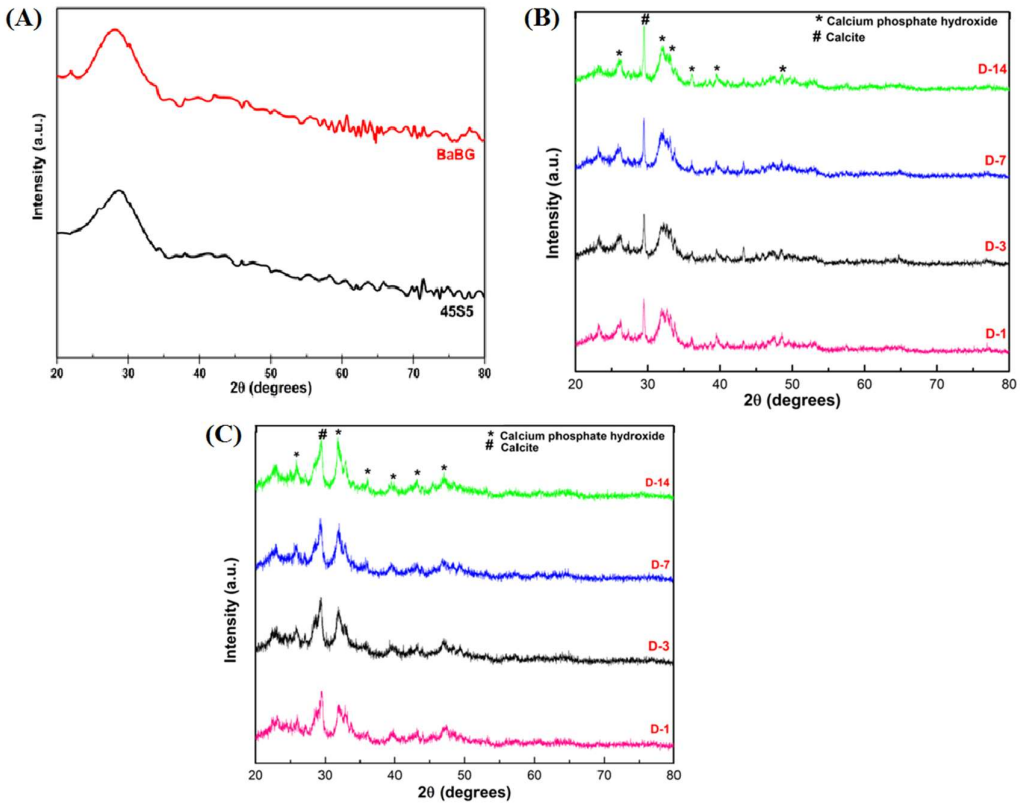

Figure 2.2: XRD pattern of BaBG & 45S5 bioactive glass samples before SBF treatment (A) and XRD pattern of 45S5 (B) and BaBG (C) after soaking them in SBF for 1, 3, 7, and 14 days.

2.2.4. Transmission electron microscopy (TEM) analysis

The TEM image of 45S5 and BaBG samples showed heterogeneous nanosized spherical particles (**Fig. 2.4A**), and their corresponding SAED patterns obtained exhibited diffused rings without diffraction spots or well-defined diffraction rings, suggesting that the synthesized BGs are amorphous (depicted in **Fig. 2.4B**).

2.2.5. pH behavior of the bioactive glass samples in the SBF solution

The pH of the SBF solution altered after treatment with bioactive glasses for a period of 30 days which is depicted in the **Figure 2.5**. In the present study, the pH of the solution at 37°C increased gradually till the first three days, attained maxima and then

declined. It was observed that on the fourth day, the pH of the solution after immersion with 45S5 and BaBG was found to be 9.02 and 9.91 respectively in comparison to the initial pH of 7.4. Surprisingly, in the case of BaBG, the pH of SBF increased again after 12 days till day 17, followed by a gradual decrease in the pH. However, this increment in the pH was not found in the case of 45S5.

The initial increase in pH value was due to the rapid leaching out of the Na^{+}, Ca^{2+}, and Ba^{2+} ions from the glass sample in exchange with H^{+} or H_3O^{+} ions that are present in the SBF solution similarly as suggested previously (Hench 2006). The released Ca^{2+} ions stimulate the release of various growth factors like VEGF (Vascular endothelial growth factor) and FGF (fibroblast growth factor) which stimulate angiogenesis (Ajita, Saravanan et al. 2015). The acidic H^{+} ions are then replaced by various cations present in the bioactive glasses which increase the level of hydroxyl ions in the SBF solution. The hydroxyl ion attacks the silica network, resulting in silanol formation through hydrolysis. However, the pH of the solution decreased after 3 days as the concentration of cations gradually decreased on the surface of the sample. This decrease in the pH may also be caused due to the precipitation of Ca^{2+} ions as calcium phosphates which form the crystalline apatite layer as seen in SEM images (**Figure 2.6**). It has been previously reported that the apatite formed on the surface of the bioactive glass samples prevents the direct contact of the glass surface with the SBF that may hinder the ionic exchange so the pH decreases (Tripathi, Rath et al. 2019).

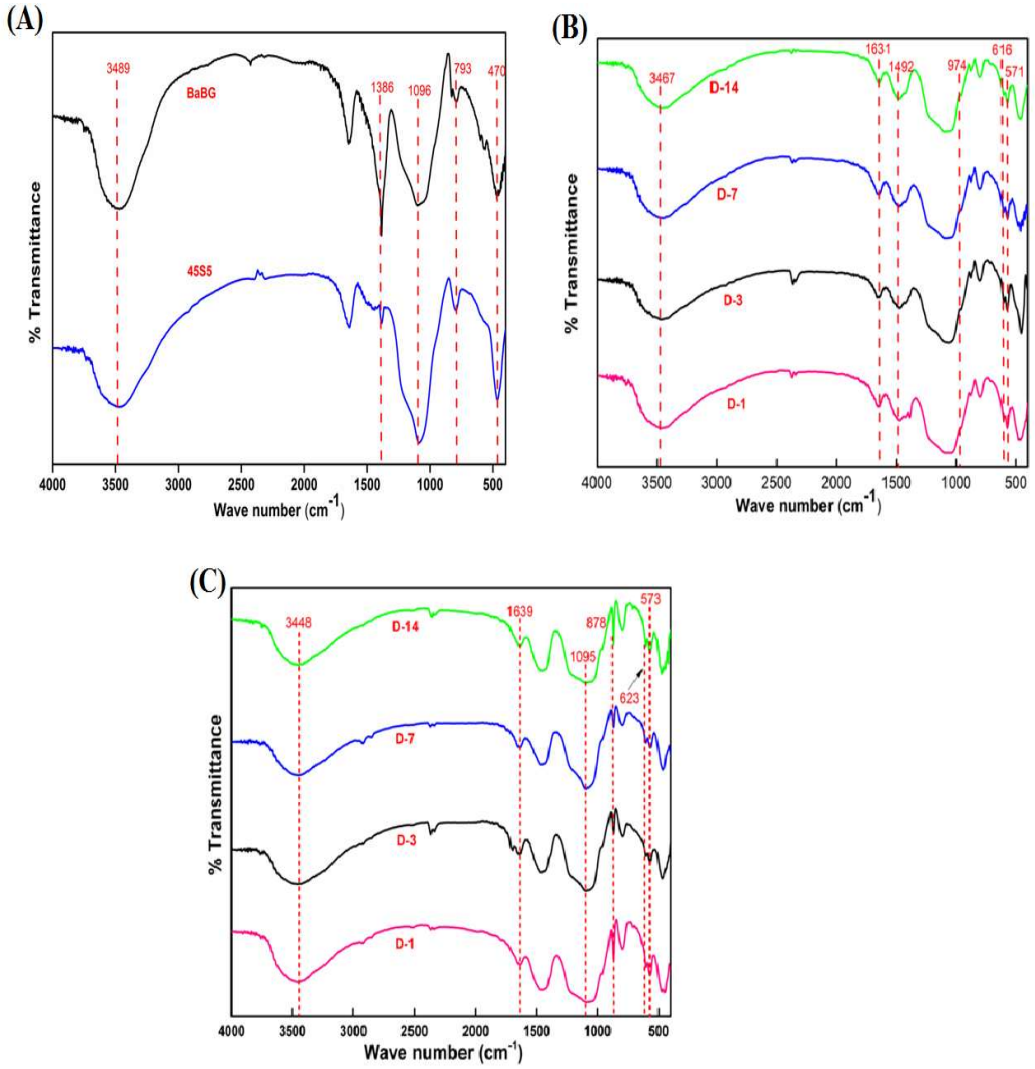

Figure 2.3: FTIR transmittance spectra of the bioactive glasses before soaking it in SBF solution (A) and FTIR spectra of 45S5 (B) and BaBG (C) after immersion in the SBF solution for 1, 3, 7, and 14 days.

In BaBG, the rise in pH of the SBF was more compared to 45S5 due to higher NBO (nonbridging oxygen) to which the protons from SBF bind to form silanol groups, thus enhancing the faster deposition of hydroxycarbonate apatite (Ali, Ershad et al. 2018). Earlier studies have also reported that the substitution of barium oxide at the expense of silica possesses a higher rate of dissolution (Arepalli, Tripathi et al. 2015) and hence greater bioactivity (Leenakul, Kantha et al. 2013). Brukner et al., (Brückner, Tylkowski

et al. 2016) investigated the effects of substitution of alkali ions of varying ionic radius in the basic glass structure and reported that substituting with ions of the larger ionic radius caused expansion of the glass network and hence decreased oxygen density. Thus, the incorporation of Ba^{2+} (ionic radius = 135 pm) substituting for Ca^{2+} (ionic radius = 100 pm) in bioactive glass enhances ion exchange which raises the pH of SBF.

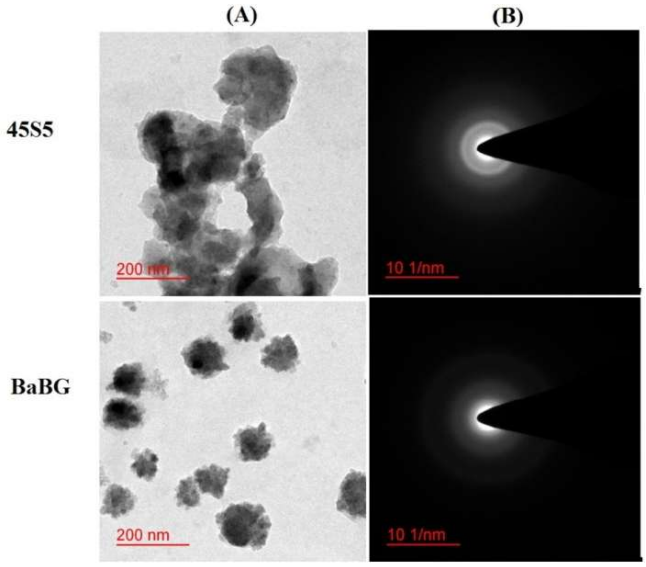

Figure 2.4: The morphology and phase analysis of the synthesized BaBG and 45S5. (A) TEM image and (B) SAED pattern of 45S5 and BaBG

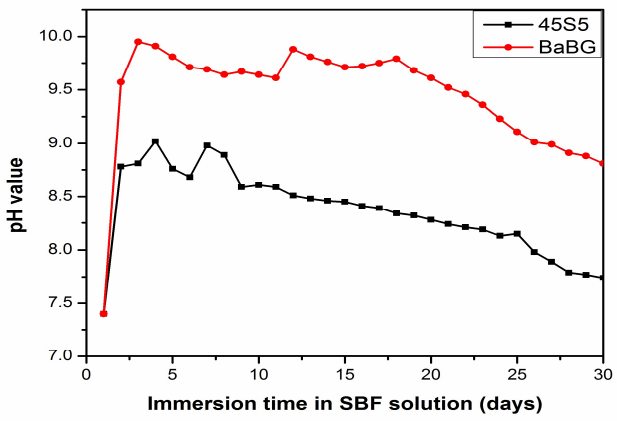

Figure 2.5: The changes in the pH of the SBF solution after soaking BaBG and 45S5 for 30 days

2.2.5. SEM and EDX analysis of BaBG and 45S5

The SEM micrograph displays the surface morphology of the bioactive glass before and after the SBF treatment for 1, 3, and 14 days at 37°C as shown in **Figure 2.6**. 45S5 and BaBG bioactive glasses showed very fine scattered grains on their surface before their treatment with SBF (**Figure 2.6(i)**) which was similarly observed by Beherei et al., (Beherei, Mohamed et al. 2009) with no existence of HA particles. Moreover, the elemental analysis by EDX confirms the substitution of Ba in the BaBG along with the presence of other elements like Ca, Si, and P in both the bioactive glasses as shown in **Figure 2.7(iA & iiA)** respectively. Subsequently, the surface of the SBF-treated 45S5 was covered with a layer of irregular crystals of various shapes and sizes that continued to grow with increasing time duration (**Figure 2.6(ii)**). The crystals formed are due to the deposition of HA which was also confirmed by the XRD and FTIR results. Similarly, **Figure 2.6(iii)** shows the partial formation of needle-shaped crystals after 1 day on BaBG following treatment with SBF. Gradually the entire surface was covered by a layer of the *in-situ* formed HA (Shahrbabak, Sharifianjazi et al. 2019). The EDX analysis also confirmed the formation of HA on the surface of 45S5 and BaBG (**Figure 2.7(iB & iiB)**). Recent studies have demonstrated that the formation of HA largely relies on the exchange of cations of the bioactive glasses that act as network-modifying agents and the H^+ from the SBF (Baino 2019). Further, there is adsorption of ions (Ca^{2+} and PO_4^{3-}) from SBF. Hence, we may conclude that both the bioactive glasses favor the growth of HCA upon SBF treatment as also confirmed by the FTIR as well as XRD.

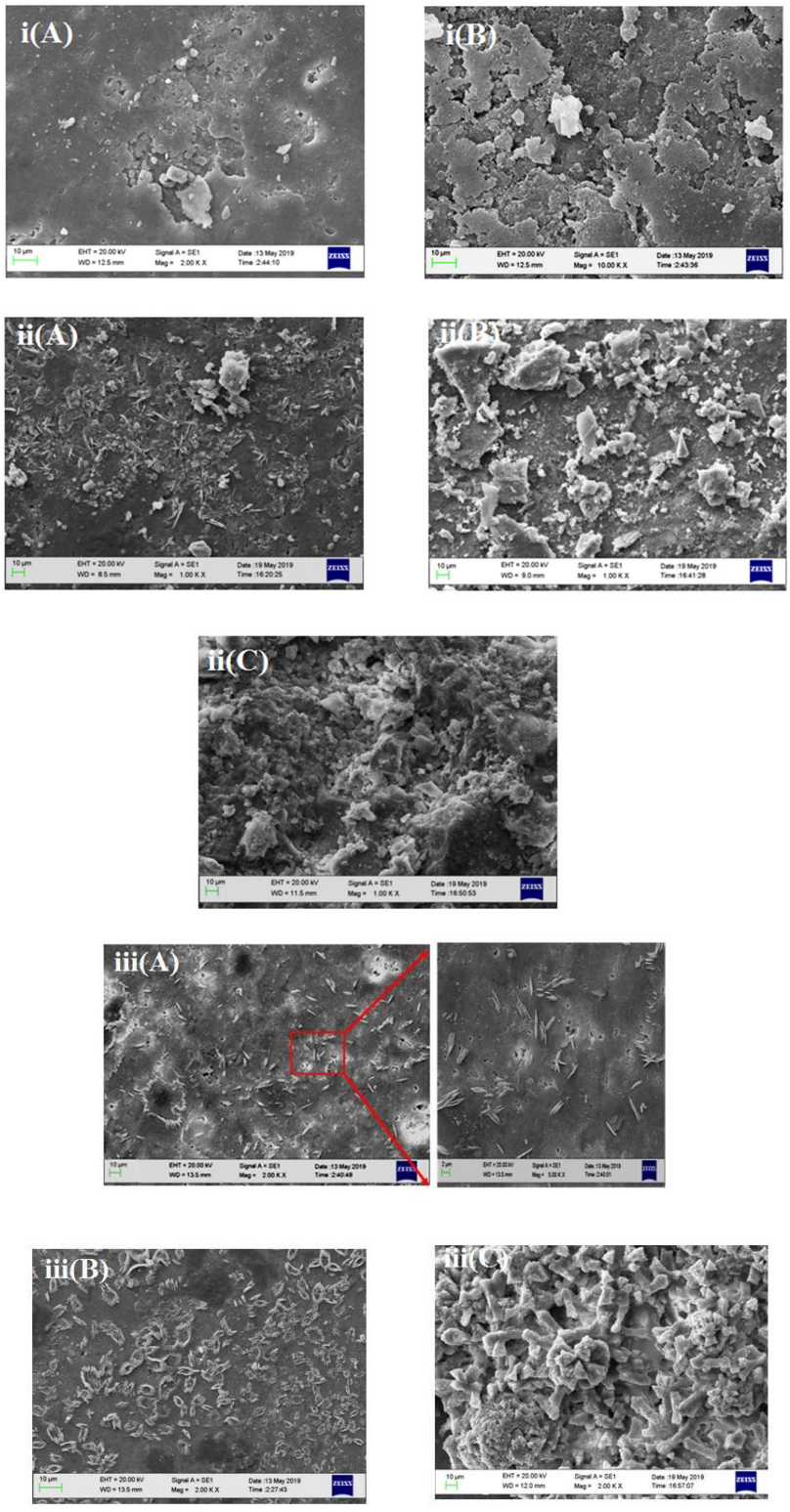

Figure 2.6: SEM micrographs of (i) 45S5 (A) and BaBG (B) before immersion in SBF, (ii) 45S5 and (iii) BaBG after the SBF treatment for 1 (A), 3 (B), and 14 (C) days respectively

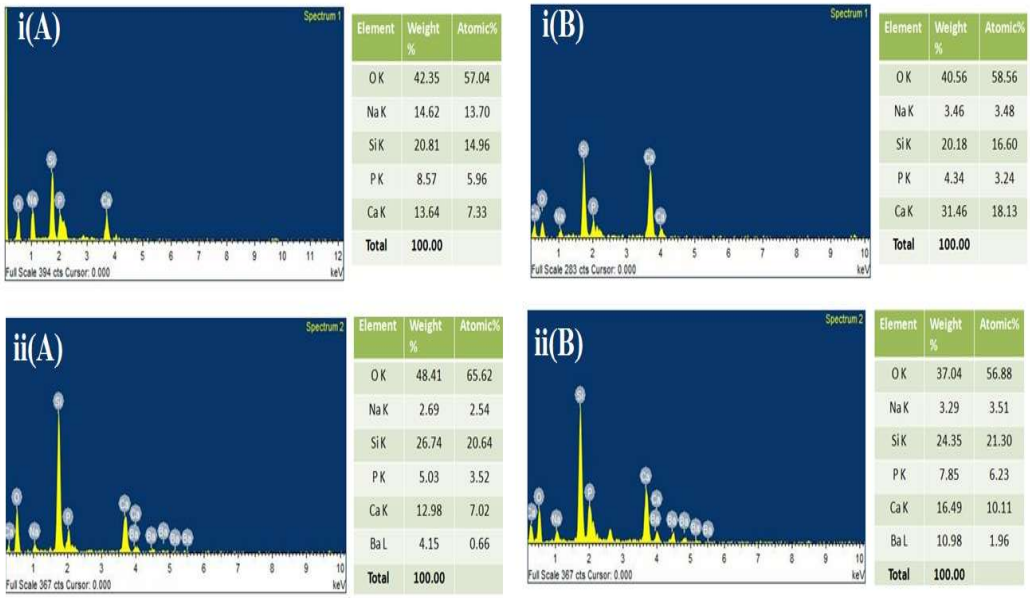

Figure 2.7: EDX analysis of (i) 45S5 and (ii) BaBG after 1 (A) and 14 (B) days of SBF treatment.

2.2.6. BaBG and 45S5 shows biocompatibility in hemolysis assay

Hemolysis is the lysis of the cytoplasmic membrane of RBC and the release of oxygen-containing protein i.e. hemoglobin into the blood plasma. It is an indicative phenomenon which occurs when any toxic foreign material comes in contact with the blood (Seyfert, Biehl et al. 2002). Thus, hemolysis assay is an important parameter to analyze the biocompatibility of any synthesized material with blood so that it can be used as an implant material. The percentage of hemolysis of the blood caused by the treatment of BaBG and 45S5 is represented in **Figure 2.8**. It was observed that the hemolysis index increased with the increase in the amount of BaBG and 45S5. However, 45S5 causes maximum hemolysis of 3.21 ± 0.28% while BaBG caused hemolysis of 2.91± 0.39% when 100 mg was used which is under the permissible limit of 5% (Rathinam, Sivakumar et al. 1994). Thus, the hemolysis assay ascertains the

biocompatibility and non-hemolytic nature of the bioactive glass samples. Hence, BaBG and 45S5 have medically high potential to be used as a regenerative biomaterial.

2.2.7. BaBG and 45S5 exhibit cytocompatibility during *in vitro* cell proliferation and cytotoxicity assay

In the present study, the glioblastoma (C6 cells) cells that are adherent in nature were used to evaluate the cytocompatibility while human leukemic suspension-type cells of granulocytic origin (K562 cells) were used to assess the biocompatibility of the bioactive glasses. These cells are immortal, unlike the primary glial cells that have a limited life. Normally, the majority of the synthesized biomaterials exhibit cytocompatibility with various cell lines but their effects at higher concentrations need longer incubation to obtain better knowledge about cell proliferation and viability. Thus, the above cancerous cell lines were used which have uncontrolled cell division.

The concentration-dependent effect of BaBG and 45S5 on the *in vitro* proliferation and cytotoxicity were performed on the K562 cells and are represented in **Figure 2.9(A, B)**. The cells were incubated with different concentrations of BaBG and 45S5 ranging from 5 µg/ml to 100 µg/ml. In the case of the *in vitro* cytotoxicity test, K562 cells were incubated for 18 h as this time period is considered optimum, neither short nor too long (Decker and Lohmann-Matthes 1988). Studies have reported that longer incubation makes the specific release of lactate dehydrogenase (LDH) less significant (Wiltrout, Frost et al. 1978). Further, longer incubation is required to observe long-term effects like growth inhibition so the K562 cells were incubated for 48 h in case of an *in vitro* proliferation study. Statistical analysis by two-way ANOVA revealed significant differences in proliferation and cytotoxicity among the groups ([F (2, 45)=95.15;

P<0.05]) and ([F (2, 45)=1398; P<0.05]) respectively, concentration ([F (4, 45)=6.420; P<0.05]) and ([F (2, 45)=115; P<0.05]) respectively, and between group and concentration ([F (8, 45)=2.382; P<0.05]) and ([F (8, 45)=27.53; P<0.05]) respectively. Post hoc analysis revealed that there was a significant decrease in the percentage proliferation of K562 cells compared to the control group after treatment with 45S5. Similarly, to further confirm the tolerability of BaBG and 45S5, the concentration-dependent cytotoxicity test was performed which showed an increase in the % cytotoxicity with the increase in BaBG and 45S5 (**Figure 2.9B**). However, the increase in the % cytotoxicity is less than 10% for both glasses which is within the acceptable limit. In support of our result, previous studies have shown that barium did not impart any toxicity on the osteoblast cell (MG63) (Ball, Mound et al. 2014). Even Loza et al., (Loza, Föhring et al. 2016) reported barium sulfate to be an inert compound with no cytotoxic response on the alveolar macrophages. Therefore, BaBG prepared using the sol-gel method is biocompatible and tolerant to K562 cells which corroborate with the non-hemolytic nature as observed in the hemolysis assay.

Further, the time-dependent effect of BaBG and 45S5 on the percentage cell proliferation was assessed on the C6 cells at different time intervals (24, 48, 72, and 96 h) shown in **Figure 2.9C**. The incubation of the C6 cell line with BaBG and 45S5 at a fixed concentration of 50 µg/ml showed a significant increase in percentage cell proliferation among the group ([F (2, 24) = 23.90; P<0.05]) but not with time ([F (3, 24) = 1.323; P<0.05]). However, there was a significant interaction between group and time ([F (6, 24) = 4.111; P<0.05]). Post hoc analysis revealed that BaBG induced an increase in percentage proliferation in the C6 cell line compared to the control from 72 h onwards. This increase in percentage proliferation may be due to the doping of barium

as this effect was not observed with the 45S5 treatment. In support of our findings, previous reports demonstrated that the incorporation of divalent ion promotes cell proliferation by enhancing cellular activity (Zhu, Lu et al. 2019). Overall, BaBG showed biocompatibility and cytocompatibility in concentration and time-dependent manner for K652 and C6 cell lines respectively. Surprisingly, the increased proliferating effect of BaBG was more specific to C6 glial cells. This may be due to the barium ion as the activity of glial cells is largely influenced by the ion exchange mechanism (Kivi, Lehmann et al. 2000).

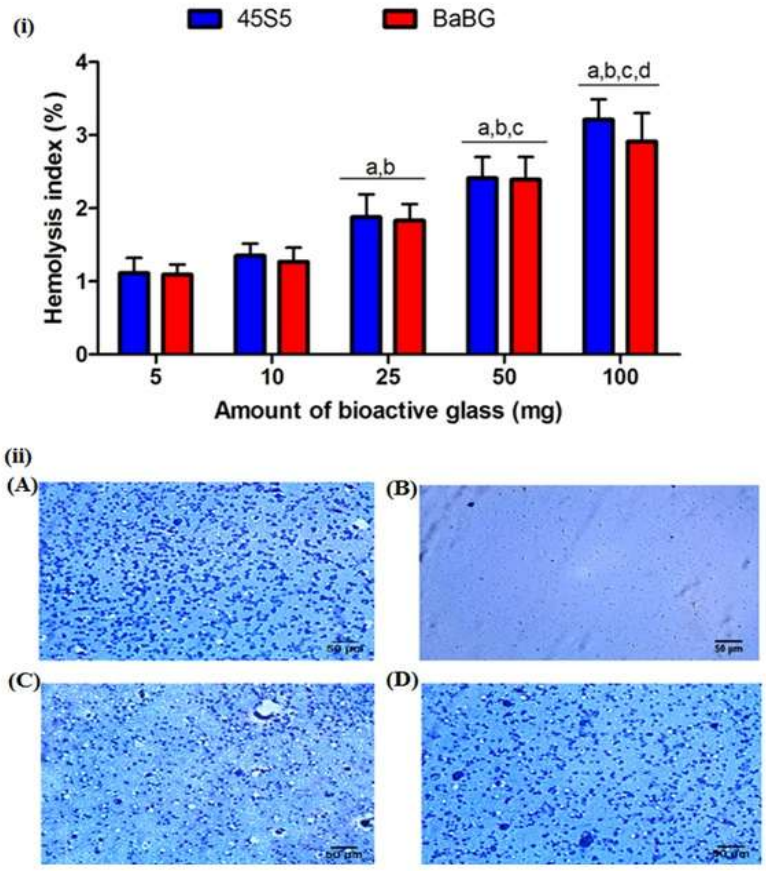

Figure 2.8: Effect of BaBG & 45S5 sample on hemolysis at different concentrations (i) and micrographs of RBC cells after incubation with negative control (A), positive control (B), 45S5 (C) and BaBG (D) respectively. All values are mean ± SD (n=4). $^{a}p<0.05$, $^{b}p<0.05$, $^{c}p<0.05$ and $^{d}p<0.05$ compared to 5, 10.25 and 50 mg respectively. (Two-way ANOVA followed by Bonferroni post hoc test)

2.2.8. BaBG and 45S5 exhibits cytocompatibility during acridine orange/ethidium bromide staining

The use of biomaterials at higher concentrations always increases the chances of cytotoxicity so the *in vitro* cytocompatibility of BaBG and 45S5 was further elucidated in the adhered cell line i.e. C6 through the apoptotic assay (acridine orange/ethidium bromide) (**Figure 2.10**). Apoptosis is one of the crucial parameters for the assessment of the cytocompatibility of novel compounds. In this study, the apoptosis was determined by the differential uptake of acridine orange and ethidium bromide by the C6 cells. Acridine orange is a nucleic acid intercalating fluorescent dye that emits uniform green fluorescence by both viable and nonviable cells. Since apoptosis causes chromatin condensation followed by its fragmentation so when the cells enter the early apoptotic phase, they emit green central fluorescence (nucleus) surrounded by green patches due to the cleaved DNA. In the late apoptotic phase, the condensed DNA emits orange fluorescence as the cytoplasmic membrane of the cells is compromised so the uptake of ethidium bromide is more than the acridine orange (Baskić, Popović et al. 2006). Treatment with BaBG and 45S5 showed that most of the cells are viable as the cells emit uniform bright green fluorescence after 18h of incubation with fewer cells in the early apoptotic phase. This result substantiates the increased proliferation of C6 cells by BaBG treatment (**Figure 2.9C**). Similarly, in the previous study, it was reported that the addition of barium in porous

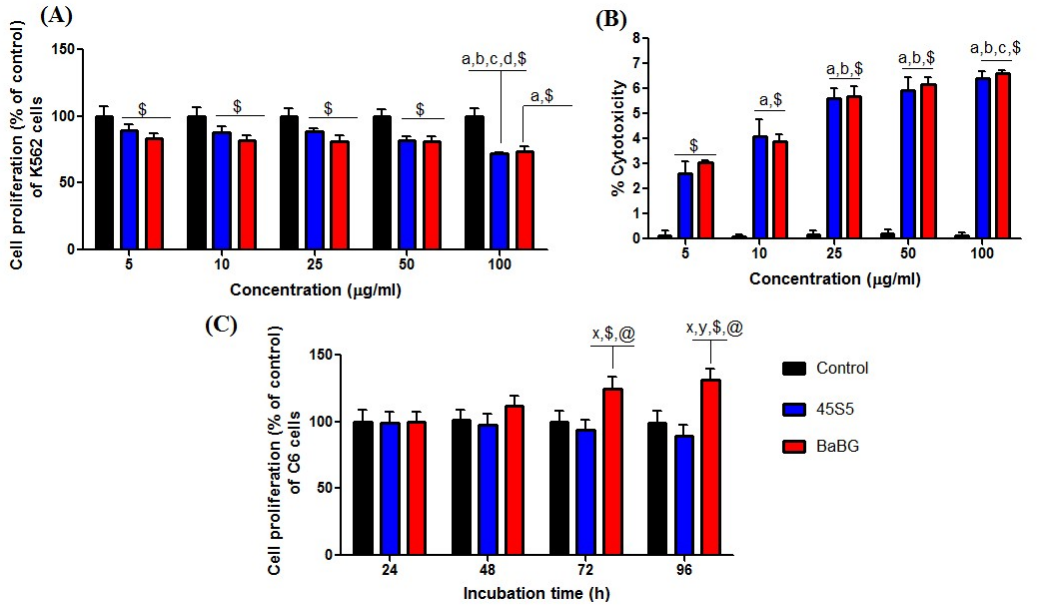

Figure 2.9: Effect of BaBG & 45S5 on percentage proliferation (A), percentage cytotoxicity of K562 cells at different concentrations (B) and percentage cell proliferation of the C6 cells at various time intervals (C). All values are mean ± SD (n=4). $^{a}P<0.05$, $^{b}P<0.05$, $^{c}p<0.05$ and $^{d}p<0.05$ compared to 5, 10, 25 and 50 µg/ml of bioactive glass sample (BaBG and 45S5), $^{x}p<0.05$, $^{y}p<0.05$ compared to 24 and 48 h of incubation with BaBG and 45S5 and $^{\$}p<0.05$ and $^{@}p<0.05$ compared to control (culture medium treated) and 45S5 treated group (Two-way ANOVA followed by Bonferroni post hoc test)

ceramic foam did not impart any toxic properties to the osteoblast cells (Ball, Mound et al. 2014). Yajima et al., (Yajima, Uemura et al. 2012) also investigated the antiapoptotic role of barium where it was found that barium increases the expression of X-linked inhibitors of apoptosis proteins (XIAP). XIAP inhibits the activation of caspase-3 and hence imparts anti-apoptotic effects. Therefore, both BaBG and 45S5 are cytocompatible.

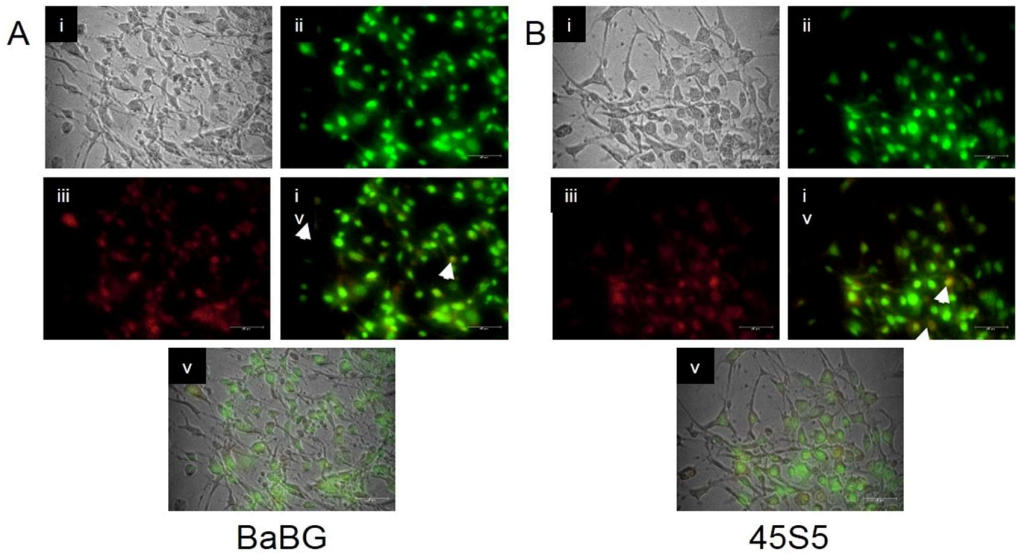

Figure 2.10: Apoptosis assay of C6 cells following treatment with BaBG (A) and 45S5 (B) with Acridine orange/ Ethidium bromide. Green color staining with Acridine orange suggests the living and healthy cells and the Ethidium bromide is staining for nucleic acid. Bright-field (i), Acridine orange staining (ii), Ethidium bromide staining (iii), the merge of ii over iii (iv), overlay of iv over i (v). Arrow indicates early apoptotic cells

2.2.9. BaBG and 45S5 shows regeneration during the scratch assay

Scratch assay is the *in vitro* technique used to analyze the effect of any synthesized compounds on cell migration. It is also an *in vitro* transection model for neurotrauma i.e. traumatic brain injury (TBI) that is the main cause of mortality in all age groups (Kumaria 2017). In this study, the wound was induced by scratching the monolayer of cells and the treatment with BaBG and 45S5 caused coordinated horizontal cell movement (**Figure 2.11A**). Statistical analysis by repeated measure two-way ANOVA revealed significant differences in percentage wound area recovery among groups [$F(3, 32)=1299$; $P<0.05$], time [$F(3, 32)=328.7$; $P<0.05$] and a significant interaction between groups and time [$F(9, 32)=135.6$; $P<0.05$]. Post-hoc analysis showed that 45S5 treatment ameliorated the percentage wound area recovery significantly compared to the culture media treated group after 4h incubation whereas BaBG

exhibited significant recovery after 16 h (**Figure 2.11B**). However, the extent of the percentage wound area recovery of 45S5 and BaBG was comparable after 24 h incubation. In support of our observation, previous reports showed that 45S5 enhances the migration of epithelial cells and also causes vascularization which aids in wound healing (Zeng, Han et al. 2015). The horizontal cell migration is considered as gold standard for the repair and regeneration of the injured tissues (Grada, Otero-Vinas et al. 2017). In addition, Zhang et al., (Zhang, Niu et al. 2018) also demonstrated that the ionic products of bioglass enhanced the proliferation of stem cells which aids in tissue regeneration. For the first time, it is reported that the inclusion of barium in bioglass showed time-dependent wound area recovery that is comparable to 45S5. In support of our finding, previously, it has been demonstrated that the combination of ions activates various extracellular signaling pathways which facilitates the migration of cells and hence helps in regeneration (Yamaguchi‐Ueda, Akazawa et al. 2019). It is also reported that the ionic product of biomaterials influences the osteoblast proliferation and recovery of tissue injury through various cytokines released from immune cells (Chen, Wu et al. 2014). Moreover, Temozolomide (TMZ), a negative control that was used in our study on C6 cells showed a significant reduction in the percentage of wound area recovery compared to the groups treated with culture media and the bioactive glass samples as it is the alkylating agent and the first-line treatment for glioblastoma.

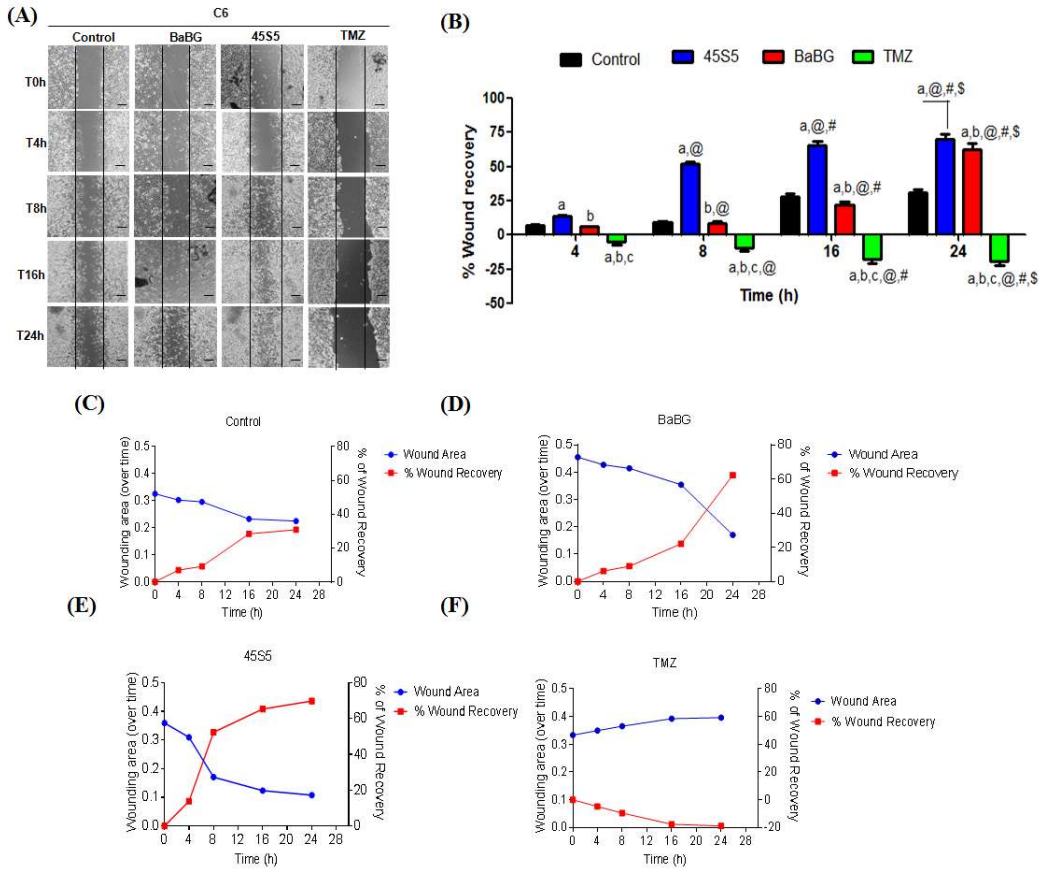

Figure 2.11: Scratch/wound healing assay in C6 cells following treatment with BaBG, 45S5, or Temozolomide (TMZ) (A), time-dependent percentage wound recovery in C6 cells treated with the above formulations (B) and comparison of time-dependent percent wound area recovery to wound area created in the presence of culture medium, BaBG, 45S5 or TMZ (C-F). All values are mean ± SD (n=3). $^{a}P<0.05$, $^{b}P<0.05$ and $^{c}p<0.05$, compared to culture media, 45S5 and BaBG treatment and $^{@}p<0.05$, $^{\#}p<0.05$ and $^{\$}p<0.05$ compared to 4, 8 and 16 h of incubation of C6 cells (Two-way ANOVA followed by Bonferroni post hoc test)

2.2.10. BaBG and 45S5 exhibits anti-inflammatory properties

Chronic and acute inflammatory diseases are associated with elevated pro-inflammatory cytokines like IL-6 and TNF- α as an inflammatory response which leads to neurodegeneration (Smith, Das et al. 2012). Since the microglia are the resident immune cells of the brain and that is activated in response to traumatic events or stimuli leading to the production of pro-inflammatory mediators (Boehler, Graham et al. 2011).

Therefore, in our present study, we investigated the anti-inflammatory effects of BaBG and 45S5 in LPS-stimulated C6 cells (**Figure 2.12)**. Statistical analysis by two-way ANOVA revealed significant differences in IL- 6, TNF- α and IL- 10 level among groups ([F (1, 56)=138.3; P<0.05], [F (1, 56)=70.03; P<0.05] and [F (1, 56)=179.7; P<0.05] respectively), with different concentration of BaBG and 45S5 ([F (13, 56)=228.9; P<0.05], [F (13, 56)=513.5; P<0.05] and [F(13, 56)=279.0; P<0.05] respectively) and a significant interaction between groups and different concentration ([F (13, 56)=12.31; P<0.05], [F (13, 56)=3.797; P<0.05] and [F (13, 56)=6.839; P<0.05] respectively). Post-hoc analysis showed that LPS treatment significantly increased the levels of IL-6 and TNF- α , while it decreased the level of IL-10 as compared to vehicle (culture media) treated cells (shown in Fig. 11). The LPS-induced release of the inflammatory cytokines may be due to the activation of the microglia which leads to the progression of various chronic inflammatory diseases (Xing, He et al. 2018). Therefore, the elevation of the inflammatory mediators is a key marker for the traumatic insult of the tissues. In this regard, previously it has been reported that IL-6 and TNF- α prevent osteoblast proliferation and thus have a deleterious effect on osteogenesis as well as caused cognitive deficits in rats (Lorenzo 2000). Interestingly, treatment with BaBG and 45S5 ameliorated the LPS-induced increase in inflammatory cytokines like IL-6 and TNF- α with subsequent elevation in the anti-inflammatory cytokine i.e. IL-10 in C6 cells. However, BaBG-induced amelioration of the inflammatory response was more significant compared to 45S5. For the first time, we reported that BaBG maintained the cytokine homeostasis by alleviating the pro-inflammatory cytokines with a simultaneous increase in the anti-inflammatory mediators. Thus, BaBG can be used as a disease-modifying agent for traumatic injury.

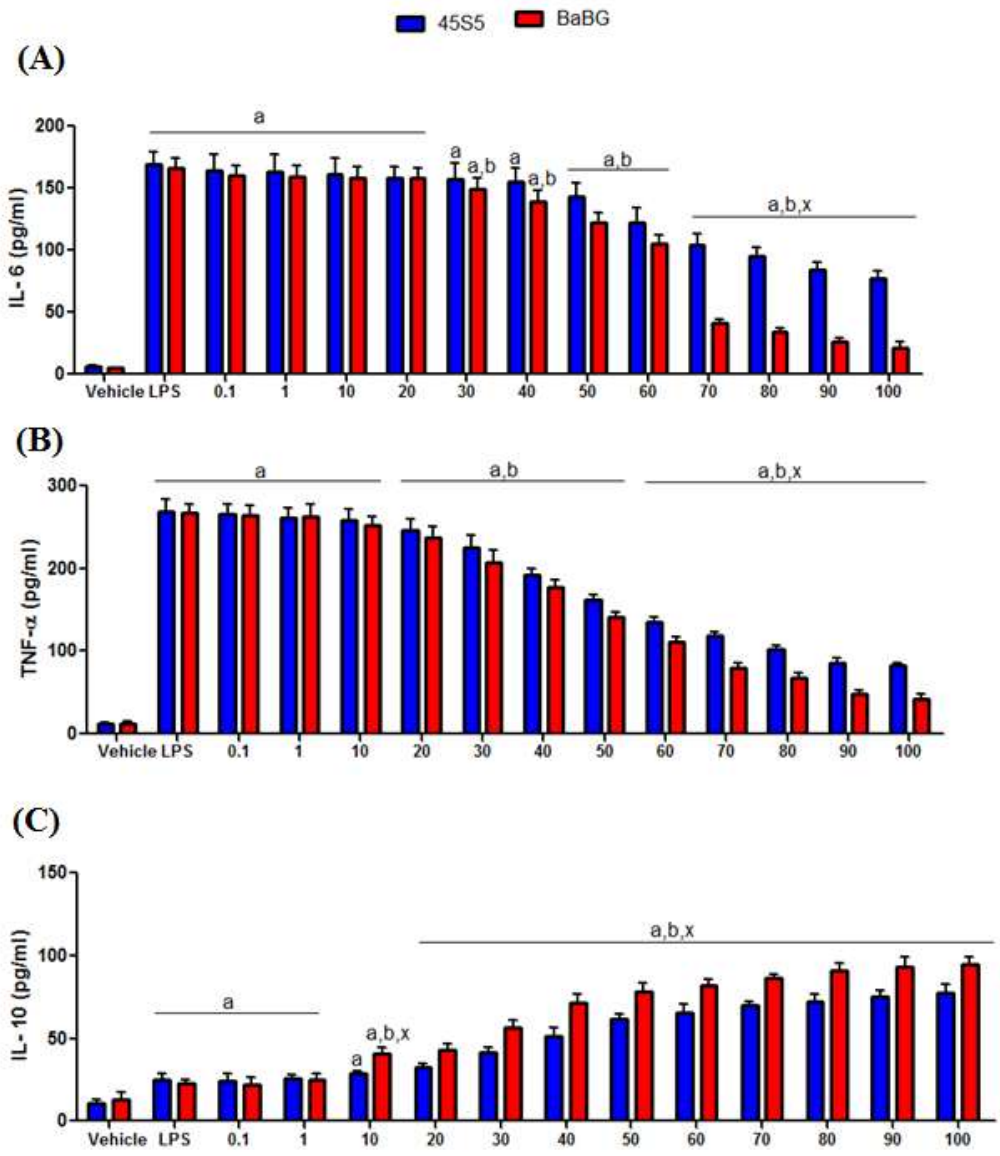

Figure 2.12: Effect of BaBG and 45S5 on IL-6 (A), TNF-α (B) and IL-10 (C) level in C6 cells. All values are mean ± SD (n=3). $^{a}P<0.05$, $^{b}P<0.05$ and $^{x}p<0.05$ compared to vehicle (culture media treated), LPS, and 45S5 treatment groups (Two-way ANOVA followed by Bonferroni post hoc test)

2.3. Conclusion

In the current investigation, a comparative study of the barium-doped bioactive glass (BaBG) and 45S5 was performed as represented in **Table 2.3**. Both the samples were prepared using the sol-gel method and characterized by XRD, SEM, EDX, and FTIR

analysis. The bioactive glasses were amorphous in nature and showed a higher tendency to form hydroxyapatite which affirms the bioactivity of the biomaterials. Further, BaBG and 45S5 were biocompatible as confirmed by the hemolysis assay. Additionally, both the bioactive glasses increased the horizontal cell migration in the scratch assay which is a gold standard for the repair and regeneration of the injured tissues. BaBG and 45S5 increased the percentage of cell proliferation without producing any cytotoxic effects on C6 and K562 cells. Moreover, BaBG exhibited prominent anti-inflammatory effects compared to 45S5. Therefore, BaBG shows potential to be used as a regenerative biomaterial in traumatic injuries.

Table 2.3: Comparison of the important properties of 45S5 and BaBG.

Sl. No.	Properties	45S5	BaBG
1	Composition (mol%):		
	SiO_2	46.1	44.85
	P_2O_5	2.6	2.60
	Na_2O	24.4	24.30
	CaO	26.9	26.90
	BaO	0.0	1.35
2	Particle size (nm)	430±41.9	508±39.3
3	BET-specific surface area (m^2/g)	20.371	18.029
4	Hemolytic index (%) of 100 mg sample	3.21±0.28	2.91±0.39
5	Cytotoxicity (%) of K562 cells at 100 µg/ml	6.39±0.27	6.62±0.08
6	Proliferation (%):		
	• K562 cells after 18 h incubation at 100 µg/ml	72.35±0.712	73.83±3.89
	• C6 cells after 96 h incubation at 50 µg/ml	89.16±8.120	131.231±8.37
7	Wound closure (%) in scratch assay after 24 h incubation	69.80±4.073	62.36±4.73
8	Inflammatory markers (pg/ml):		
	• IL-6	77.27±5.85	21.40±4.96
	• TNF- α	82.19±4.038	42.21±5.46
9	Anti-inflammatory marker (pg/ml):		
	• IL-10	77.81±4.71	94.72±4.36